Asymmetric Bioreduction of Ethyl 4-Chloroacetoacetate into Ethyl 4-Chloro-3-hydroxybutyrate by Recombinant *Escherichia coli* CgCR in Ethyl Acetate-Betaine:Lactic Acid-Water

Linsong Yang [1], Daozhu Xu [1], Luyao Jiang [2] and Yucai He [1,2,*]

[1] School of Pharmacy & School of Biological and Food Engineering, Changzhou University, Changzhou 213164, China; linsongyang@cczu.edu.cn (L.Y.); xutianjiao8@gmail.com (D.X.)
[2] State Key Laboratory of Biocatalysis and Enzyme Engineering, Hubei University, Wuhan 430062, China; 15897799515@163.com
[*] Correspondence: heyucai2001@163.com or yucaihe@cczu.edu.cn

Abstract: Objective: Optically active (*R*)-ethyl 4-chloro-3-hydroxybutyrate ((*R*)-CHBE) is a useful chiral building block for the synthesis of pharmaceuticals. Recently, there has been great interest in the synthesis of (*R*)-CHBE via the highly stereoselective bioreduction of ethyl 4-chloro-3-oxobutanoate (COBE) under mild conditions. **Methods**: A highly efficient bioreduction process for transforming COBE into (*R*)-CHBE was developed in a biocompatible organic solvent–deep eutectic solvent–water reaction medium. **Results**: Recombinant *Escherichia coli* containing carbonyl reductase (CgCR) and glucose dehydrogenase (GDH) was successfully constructed and characterized. In addition, the feasibility of the asymmetric bioreduction of COBE to (*R*)-CHBE was verified in an organic solvent–deep eutectic solvent–water (ethyl acetate-betaine/lactic acid-water) system. At pH 7.0 and 30 °C, the kinetic constants Km and kcat of COBE were 20.9 mM and 56.1 s^{-1}, respectively. A high (*R*)-CHBE yield (≥90%) was achieved by catalyzing COBE (1000 mM) in 12 h with *E. coli* CgCR cells in the presence of Ni^{2+} (7 mM) and glucose (3.5 mM glucose/mM COBE) in an ethyl acetate-betaine/lactic acid-H$_2$O (50/7/43, *v*/*v*/*v*) system. The effects of organic solvents and DESs on whole-cell permeability were analyzed. **Conclusions**: An efficient bioreduction system was constructed for biologically transforming COBE to (*R*)-CHBE via whole-cell biocatalysis, and the established bioprocess has potential application in future.

Keywords: ethyl 4-chloro-3-hydroxybutyrate; ethyl 4-chloroacetoacetate; bioreduction; deep eutectic solvent; permeability

1. Introduction

To date, the growing global chiral drug market share has attracted many researchers to engage in the research, development, and application of chiral drugs [1–5]. Chirality is one of the fundamental properties prevalent in nature, and almost all macromolecules such as sugars, nucleic acids, proteins, and cellulose involved in life activities in the body are chiral [4–10]. Chiral 4-chloro-3-hydroxybutyrate (CHBE) is one kind of important drug intermediate [11], which can be synthesized through asymmetric catalysis of chiral catalysts [12], dehalogenase catalysis, microbial asymmetric resolution, and biocatalytic asymmetric reduction [13,14]. It is well known that optically active (*R*)-CHBE is a crucial chiral synthesis agent for manufacturing (*R*)-4-amino-3-hydroxy-butyric acid, *L*-carnitine, (*R*)-4-hydroxy-2-pyrrolidone, negamycin, macrolactin A, etc. [15,16]. (*R*)-4-Amino-3-hydroxybutyric acid can be used as an anti-convulsant for the treatment of acute epilepsy caused by ketone bodies [17]. *L*-Carnitine synthesized from (*R*)-CHBE as the initial raw material is able to treat Alzheimer's disease and male infertility [18–20]. Negamycin is an effective candidate for the treatment of nonsense-related diseases [21]. (*R*)-4-Hydroxy-2-pyrrolidone, which is

known as γ-butyllactam, has cytotoxic, antitumor, and anti-inflammatory physiological activities [22]. Macrolactin A can prevent HIV replication [23].

Commercially, the synthesis of (*R*)-CHBE from prochiral ketone ethyl 4-chloroacetoacetate (COBE) is conducted using chemical catalysts containing rare metals, reducing metal catalysts with ammonia, or flammable and explosive chemocatalysts (such as sodium borohydride) [24–26]. These methods require expensive rare metals as the chemocatalysts and harsh reaction conditions, and the optical purity of the product is not high. Distinct from chemical reduction, biocatalytic reduction has mild conditions, good selectivity, and high conversion [27,28]. Using carbonyl reductase to catalyze the asymmetric bioreduction of COBE to (*R*)-CHBE is a promising approach [29]. The key to the biological reduction process is the participation of carbonyl reductase and NAD(P)H [30,31]. Presently, the coupling of reductases with dehydrogenases for the regeneration of coenzyme can be applied to enhance bioreduction [32]. Glucose dehydrogenase (GDH) enables the biological transformation of glucose to gluconic acid, promoting the biotransformation of $NAD(P)^+$ to NAD(P)H (Figure 1).
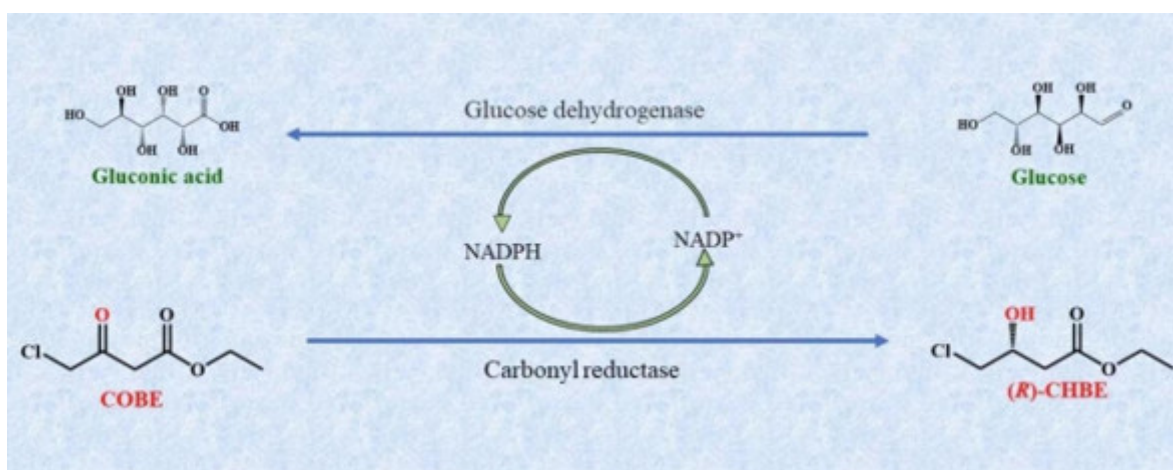

Figure 1. Glucose/GDH cofactor regeneration system.

It is known that the substrate COBE is a hydrophobic compound that is insoluble [33]. In the bioprocess of whole-cell catalysis, a high titer of the hydrophobic substrate may inhibit the biocatalytic efficiency in the whole-cell reaction [34–36]. The supply of hydrophobic organic solvents to the biocatalytic system can enhance the efficiency of the bioreaction [37–40]. Deep eutectic solvents (DESs), which can be prepared by blending a hydrogen-bond-acceptor (e.g., choline chloride) and a hydrogen-bond-donor (e.g., amines, carboxylic acids, and polyols) [41–43], are recognized as green solvents. They have been extensively utilized as a chemical or biochemical reaction medium for enhancing catalytic efficiency [44–47]. Some DESs have been applied as a tool for biocatalysis, either as solvents or as separative agents to overcome challenging workup procedures [48–50]. Many organic solvents and DESs have been applied for enhancing the availability of insoluble substrates, alleviating the inhibition of the substrate, and promoting the biocatalytic efficiency [51]. The use of additives (organic solvents and DESs) might be applied to increase the permeability of cell membranes for facilitating the efficiency of substance exchange during biocatalytic reactions [52].

Due to the coenzyme dependence of keto reductase in the bioreduction of COBE, it is generally necessary to supply NAD(P)H to the bioreaction system [52–54]. To reduce the performance cost, co-substrate glucose can be supplied to the COBE-reducing system to yield (*R*)-CHBE using tandem dehydrogenase and other coenzymes [55–57]. Compared to the purified enzymes, whole-cell bioreduction has gained much attention, and it avoids the complicated step of enzyme purification and facilitates product recovery [58–60]. In an ideal bioreduction system, carbonyl reductase coupled with dehydrogenase for cofactor

regeneration in the same kind of bacterial cells is a good strategy for bioreduction. This strategy can be applied to biologically reduce COBE to (*R*)-CHBE with high activity and substrate-tolerance of the biocatalyst, which has the potential to replace traditional chemical reduction processes [61–64].

Organic solvents and DESs can enhance the biocatalytic efficiency [28,37,49]. In a previous report [44], DES betaine/lactic acid (1:2, mol/mol) was shown to be highly biocompatible as a biocatalyst. Thus, an attempt might be made to combine organic solvents and betaine/lactic acid as a reaction medium for the bioreduction of COBE. The constructed bioreaction system might facilitate the dissolution of COBE, which would be suitable for biocatalysts to participate in the bioreduction of COBE. In this study, (*R*)-CHBE was synthesized from COBE by newly constructed recombinant *E. coli* CgCR cells expressing carbonyl reductase (CgCR) and glucose dehydrogenase (GDH). Whole-cell bioreduction factors (temperature, pH, substrate concentration, co-substrate, metal ions, etc.) for assessing the biocatalytic activity were examined in an organic solvent-betaine/lactic acid-water system. An efficient whole-cell biotransformation of COBE to (*R*)-CHBE was successfully established in a sustainable bioreaction system.

2. Materials and Methods

2.1. Chemicals

Yeast extract, glucose, betaine, lactic acid (LA), methyl isobutyl ketone, COBE, ethyl acetate, NADPH, acetic anhydride, and other reagents were purchased from Maclin, Ltd. (Shanghai, China).

2.2. Synthesis of DES Betaine/Lactic Acid

Betaine and lactic acid were blended in a ratio of 1:2 (mol/mol) under agitation at 300 rpm under 80 °C until the solution became clear and transparent.

The Kamlet–Taft parameter measurement method of betaine/lactic acid refers to Xia's research [65]. K-T solvatochromic parameters were measured using Nile red (NR), *N,N*-diethyl-4-nitroaniline (NEt2), 4-nitroaniline (NH₂). NH₂ and NEt2 were used to assay β and π*, respectively. NR was utilized as a solvent color indicator to calculate the α value. The dyes were separately dissolved in methanol and stored in brown reagent bottles. An amount of 5 mL of dye solution was added to a 5 mL centrifuge tube, and dried and evaporated in vacuo at 40 °C for 48 h. Then, 3 mL of betaine/lactic acid was put into the dried dye, and the mixture was transferred to a 1 cm² quartz cuvette. The absorption spectrum of the prepared mixture was measured at room temperature in the wavelength range of 300–700 nm using a UV/Vis spectrophotometer (TU-1900, Beijing Purkinje General Instrument Co., Ltd., Beijing, China).

The α, β, and π* values were calculated as follows, respectively:

$$\pi^* = 0.314 \times (27.52 - v_{NEt2}) \tag{1}$$

$$\beta = 11.134 - \frac{3580}{\lambda(NH_2)_{max}} - 1.125\pi^* \tag{2}$$

$$\alpha = \frac{19.9657 - 1.0241\pi^* - v_{NR}}{1.6078} \tag{3}$$

where π* is normalized to give cyclohexane and DMSO, λ_{max} is the wavelength corresponding to maximum absorption of the dye, and $v = 1/(\lambda_{max} \times 10^{-4})$.

2.3. Construction and Expression of Reductase

The genes of reductase (CgCR) from *C. glabrata* CGMCC 2.234 and glucose dehydrogenase (GDH) from *B. megaterium* (BmGDH) (GenBank: SUV21072.1) were co-expressed in one *E. coli* cell (Figure 2). pRSF-F (AGCCAGATCCGAATTCGAGC) and pRSF-R (GTG-GTGATGATGGATGGCTGC) were applied to linearize pRSFDuet-1 backbone. Primers

CgCR-R (ATTCGGATCCTGGCTTTACACAAATGGCTTAAATGGCCCCC) and CgCR-F (CACCATCATCACCACATGGCTGCTCTACATAAGAACACTTCTACTTTG) were applied to amplify CgCR. Primers GDH-R (GATATATCTCCTTAGGTACCTTACACAAATGGCT-TAAATG) and GDH-F (CACCATCATCACCACATGGCTGCTCTACATAAGAACACTTC) were applied to amplify GDH. The purified CgCR, GDH, and linearized pRSFDuet-1 fragments were linked using T5 exonuclease by transforming *E. coli* DH 5α chemically competent cells. The pRSFDuet-CgCR-GDH was verified through DNA sequencing, and it was transferred into competent *E. coli* BL21 (DE3) through electroporation to give recombinant strain *E. coli* CgCR. The plasmid with correct gene sequencing expression was introduced into the BL21 clone strain for expression. Under the action of IPTG inducer, it promoted the expression of target genes. The nucleic acid and SDS-PAGE electrophoresis were used to examine the expression results.
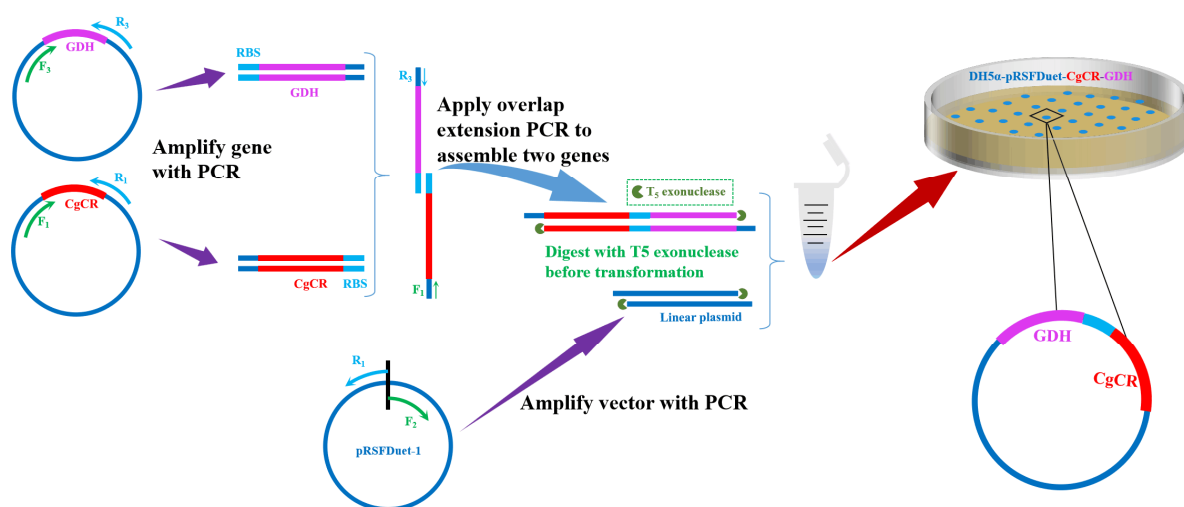

Figure 2. Construction process of recombinant *E. coli* CgCR.

Recombinant *E. coli* CgCR was inoculated, cultivated, and harvested as previously reported [53]. The activity of reductase in *E. coli* CgCR was spectrophotometrically measured under pH 7.0 and 30 °C by detecting the alteration in NADPH absorbance (340 nm) in a total volume of 1 mL containing 0.2 mM NADPH, a different concentration of COBE, 0.85 mL buffer (100 mM KPB), and 100 μL crude enzyme. One unit (U) of enzyme activity of CgCR was defined as the enzyme amount (mg protein) that can oxidize 1 μmol of NADPH per minute under the specified conditions.

2.4. Bioreduction of COBE with CgCR Cell in Water System

Several bioreaction factors were assessed in the biotransformation of COBE into CHBE. To test the effect of reaction temperature on the bioreduction, bioconversion was performed at various temperatures (15–55 °C) in the aqueous system containing glucose (1 mM glucose/mM COBE), COBE (100 mM), and CgCR cells (OD_{600} = 100). To examine the effect of medium pH on the bioreduction, bioconversion was performed at 30 °C in the bioreaction system (citrate buffer solution, pH 4–5; phosphate-buffered solution, pH 6–8) containing glucose (1 mM glucose/mM COBE), COBE (100 mM), and CgCR cells (OD_{600} = 100). To assess the influence of metal ion additives on the biocatalytic efficiency, Fe^{3+}, Fe^{2+}, Ni^{2+}, Gr^{3+}, Zn^{2+}, Mg^{2+}, Ca^{2+}, Mn^{2+}, Li^{2+}, Sn^{4+}, Al^{3+}, and Sr^{3+} (6 mM) were individually supplied to the aqueous system with glucose (3.5 mM glucose/mM COBE), COBE (100 mM), and CgCR cells (OD_{600} = 100) at 30 °C and pH 7.0. To evaluate the influence of different Ni^{2+} concentrations on the biocatalytic efficiency, Ni^{2+} (0~10 mM) was added into the aqueous system (pH 7.0) containing glucose (3.5 mM glucose/mM COBE), COBE (100 mM), and CgCR cells (OD_{600} = 100) at 30 °C and pH 7.0. To test the effect of glucose ratio on the biocatalytic efficiency, different concentrations of glucose

(glucose:COBE = 0.5:1, 1:1, 1.5:1, 2:1, 2.5:1, 3:1, 3.5:1, 4:1, or 5:1, mol/mol) were individually added to the aqueous system with CgCR wet cells (OD_{600} = 100) at 30 °C and pH 7.0. To investigate the influence of substrate concentration on the biocatalytic efficiency under the above optimized system, different concentrations of substrate (100–1000 mM) were individually supplied to the 10 mL system with CgCR cells (OD_{600} = 100), glucose (3.5 mM glucose/mM COBE), and Ni^{2+} (7 mM) at 30 °C and pH 7.0. Samples were periodically withdrawn for the assay.

2.5. Bioreduction of COBE with CgCR Cells in Organic Solvent-Betaine/Lactic Acid-Water System

To enhance the productivity of (*R*)-CHBE, organic solvents were individually supplied to the bioreaction system. To evaluate the influence of organic solvent on the biocatalytic efficiency, different solvents (ethyl acetate (EA), isopropyl alcohol (IPA), butyl acetate (BA), and methyl isobutylketone (MIBK)) (50%, *v/v*) were separately added to the bioreaction system containing CgCR cells (OD_{600} = 100), glucose (3.5 mM glucose/mM COBE), COBE (100 mM), and Ni^{2+} (7 mM) at 30 °C and pH 7.0. To investigate the effect of ethyl acetate (EA) ratio on the biocatalytic efficiency, different EAs (5%, 10%, 20%, 30%, 40%, 50%, 60%, 70%, and 80%, *v/v*) were separately added to bioreaction system containing CgCR wet cells (OD_{600} = 100), glucose (3.5 mM glucose/mM COBE), COBE (100 mM), Ni^{2+} (7 mM), and betaine/lactic acid (7%, *v/v*) under 30 °C and pH 7.0. To test the effect of DES (betaine/lactic acid) on the biocatalytic efficiency, different ratios of betaine/lactic acid (1%, 2%, 3%, 4%, 5%, 6%, 7%, 8%, 9%, and 10%, *v/v*) were individually loaded into the bioreaction system containing CgCR wet cells (OD_{600} = 100), glucose (3.5 mM glucose/mM COBE), COBE (100 mM), and Ni^{2+} (7 mM) at 30 °C and pH 7.0.

2.6. Effect of Cell Permeability on the Bioreduction of COBE

To assess the effect of solvents (EA and betaine/lactic acid) on cell permeability, different loadings of solvent as additives (50 vol% for EA and/or 7 vol% for betaine/lactic acid) were applied to the bioreaction system (pH 7.0) with CgCR cells (OD_{600} = 100) for 60 min at 30 °C. Centrifugal supernatant was obtained at $8000\times g$ for 5 min. Then, the supernatant was diluted with the same ratio and the optical density was measured using an ultraviolet spectrophotometer at 260 nm and 280 nm. The CgCR cell (OD_{600} = 100) was treated using 0–90 min sonication, and 100 mM COBE was catalyzed in the above optimized system.

2.7. Analytical Method

UV-visible spectrophotometer was applied to assay the turbidity of cells. After the bioreduction at 15–55 °C for 0–12 h, the substrate COBE and product CHBE were quantified using gas chromatography. Detection conditions: GC/CP-Chirasil Dex CB was employed to analyze the chirality of the product. The chromatographic conditions were as follows: the temperature of the injector column was procedurally increased to 280 °C, held at 110 °C for 2 min, increased to 110 °C at 2 °C/min, maintained for 2 min at 126 °C, and then increased to 160 °C at 2 °C/min. The temperatures of injection port and detector were both 250 °C. The carrier gas was N_2. The formulas for calculating the CHBE yield (Y) and *e.e.* value of CHBE were as follows, respectively:

$$Y\% = C_{CHBE}/C_{COBE} \times 100 \tag{4}$$

$$ee\% = (A_R - A_S)/(A_R + A_S) \times 100 \tag{5}$$

where C_{CHBE} is the concentration of CHBE, mM; C_{COBE} is the initial substrate concentration, mM; A_R is the peak area of (*R*)-CHBE; and A_S is the peak area of (*S*)-CHBE.

3. Result and Discussion

3.1. Construction of Recombinant E. coli Expressing CgCR and GDH

It is well known that the extra supply of cofactor NADPH can promote the whole-cell bioreduction [11,27]. In order to avoid the excess supply of NADPH, reductase (CgCR) and dehydrogenase (GDH) were co-expressed to create a system to regenerate NADP$^+$ into NADPH (Figure 3a,b). The bands on SDS-PAGE (Figure 3c) indicated that the molecular weights of the expressed proteins were 43.9 kDa (CgCR) and 36.0 kDa (GDH), respectively. GDH might oxidize glucose (as co-substrate) to transform NADP$^+$ into NADPH, which would be used for catalyzing COBE into CHBE via biological reduction with CgCR.
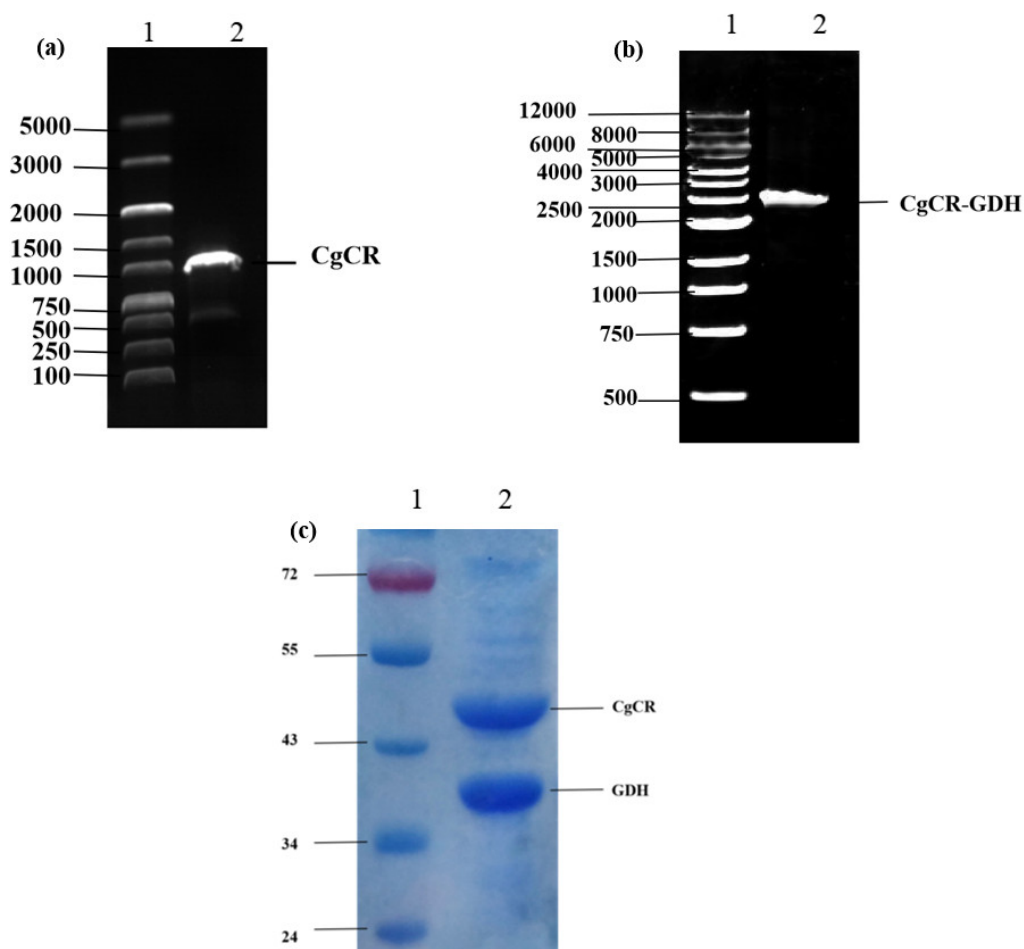

Figure 3. Analysis of the CgCR gene fragment through electrophoresis (Lane 1: marker, Lane 2: CgCR gene) (**a**); analysis of the CgCR-GDH gene fragment through electrophoresis (Lane 1: marker, Lane2: CgCR-GDH gene) (**b**); SDS−PAGE analysis of recombinant protein of CgCR and GDH in recombinant *E. coli* CgCR cells expressing carbonyl reductase (CgCR) and glucose dehydrogenase (GDH) (Lane 1: marker, Lane 2: CgCR (43.9 kDa) and GDH (36.0 kDa) in *E. coli* CgCR) (**c**).

Molecular docking (MD) can describe the interaction between molecules in depth, can visually explain the mechanism of interaction, and has become an important research method to explain the biological mechanism [27]. *CgCR* was one kind of reductase with Prelog preference in the asymmetric reduction of prochiral ketone COBE. Reductase CgCR with ligand COBE molecular docking was conducted via AutoDock and PyMOL. The interaction between CgCR and COBE is illustrated in Figure 4a,b. There was a binding energy of −12.74 kcal/mol between CgCR and COBE. The low energy facilitated the bioreduction of COBE. As presented in Figure 4b,c, the binding site of CgCR from *C. glabrata* (CGMCC 2.234) with COBE included the amino acids THR-25, TYR-63, LYS-88, TYR-206, VAL-255, ASN-157, and TRP-297, which formed an active pocket. A hydrophobic

interaction between the small molecule and VAL-255 was observed, as well as hydrogen-bond interactions with THR-25, TYR-63, ASN-157, and TRP-297. In addition, the substrate molecules also had an electrostatic interaction with LYS-88 and TYR-206. These interactions played a crucial role in the stable association between COBE and CgCR.
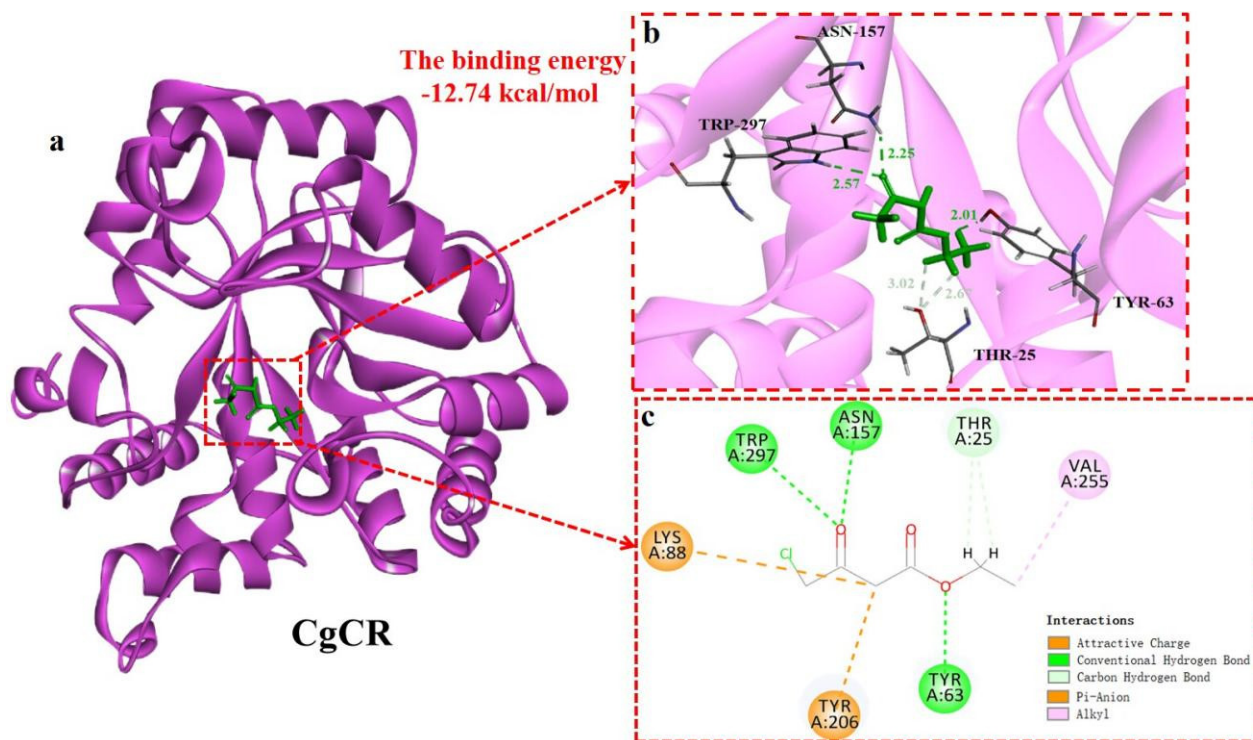

Figure 4. The binding of COBE with CgCR (**a**); making apparent interactions with the functionally important residues of CgCR (**b**); the 2D plot of CgCR binding-pocket residues and their interaction (**c**).

Bioreduction has gained extensive attention since it can be conducted under ambient conditions [38,44,66]. By altering the substrate concentration to determine the enzyme activity, the Michaelis constant Km was 20.9 mM, and Kcat was 56.1 s^{-1}. As shown in Figure 5, the feasibility of the CgCR cell to catalyze the biosynthesis of (*R*)-CHBE was verified by examining the relative activities of carbonyl reductase under the different loadings of the substrate and product. Figure 5a shows that the bioreaction activity reached the highest when NADPH (2 μmol NADPH/mol COBE) and 100 mM COBE were supplied to the bioreaction system under 30 °C and pH 7.0. As the substrate concentration increased (>100 mM), the biocatalytic activity gradually weakened due to the potential inhibition. Using 300 mM COBE as the substrate, the relative enzyme activity sharply dropped to 45.1%. When 800 mM of COBE was used as the substrate, the relative activity was below 20%. Unlike the effect of the substrate COBE on the biocatalytic reaction, the product (*R*)-CHBE had a crucial inhibitory effect on the bioreaction (Figure 5b). The inhibition of the reductase activity by product (*R*)-CHBE showed a decreasing trend. When the initial (*R*)-CHBE concentration was 5–200 mM, the activity dropped gradually. As the (*R*)-CHBE concentration continued to increase, the activity greatly declined, and the residual enzyme activity was below 45% when the (*R*)-CHBE concentration increased from 300 mM to 800 mM CHBE. Accordingly, the high substrate tolerance of CgCR cells has application potential.
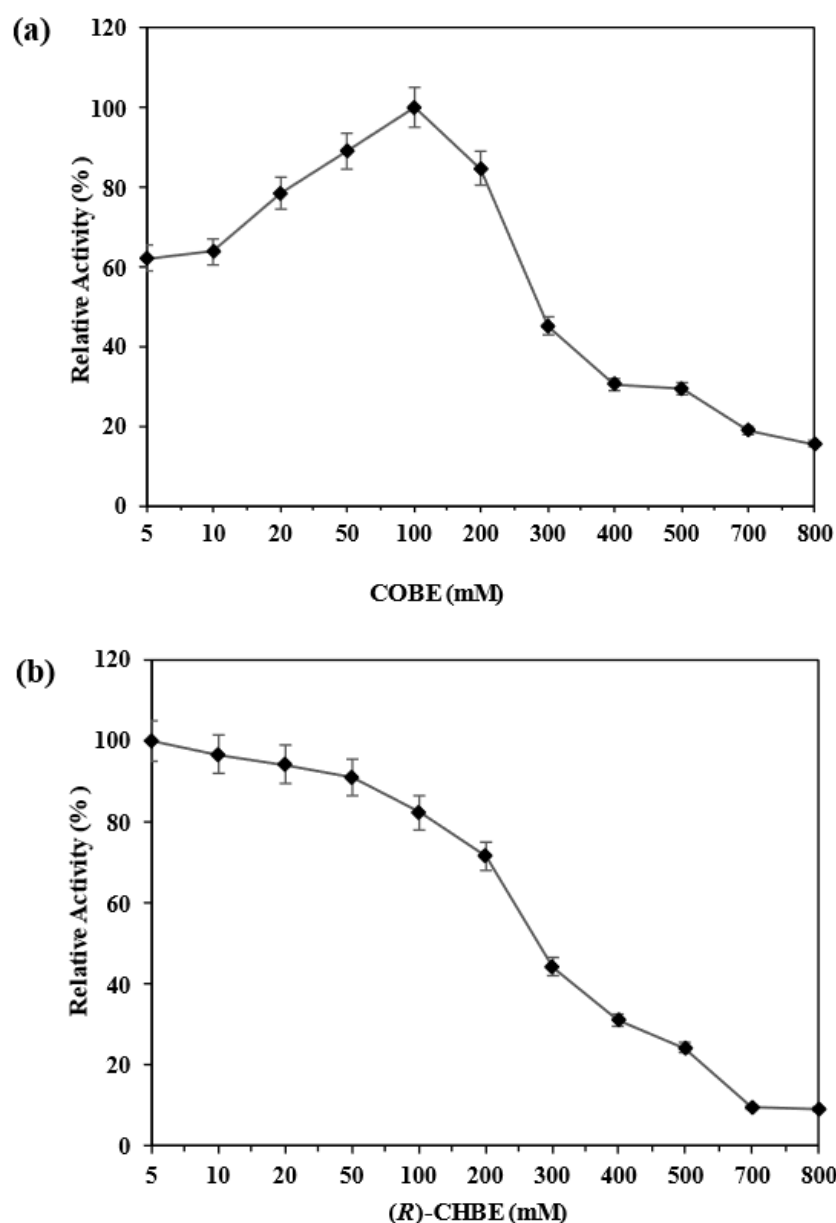
Figure 5. Effects of COBE loading (5–800 mM) on the reductase activity at 30 °C and pH 7.0 (**a**); effects of CHBE loading (5–800 mM) on the reductase activity at 30 °C and pH 7.0 (**b**).

3.2. Biotransformation of COBE in the Aqueous System

It is known that bioreduction temperature and medium pH play crucial roles in the biotransformation [38,39,67]. The influences of bioreduction temperature and medium pH on the COBE-reducing activity were investigated, and the results are displayed in Figure S1a,b (in Supplementary Materials). It was observed that bioreduction temperature apparently influenced the catalytic activity. When the temperature was increased from 15 °C to 30 °C, the COBE-reducing activities increased. At 30 °C, the highest yield of CHBE by CgCR reductase was obtained at 84.7% in 1.5 h. After the temperature exceeded 30 °C, the activities began to decrease, possibly due to the thermal deactivation of reductase in CgCR cells during the bioreduction reaction. Accordingly, the suitable temperature for promoting COBE-reducing activity was chosen at 30 °C. Under low- or high-temperature conditions, the activities decreased, so the reaction temperature should be strictly controlled during the bioreaction process. Figure 6b shows that medium pH had little influence on the bioreaction, but it generally presented a trend of rising and then falling, reaching the highest value at pH 7.0. High pH or low pH might affect the dissociation state of the

substrate and enzymes, which would influence the binding of the substrates to enzyme active centers. Clearly, recombinant *E. coli* CgCR had good pH tolerance, and the residual reductase activity reached 83.9% even at pH 4.0, indicating that CgCR reductase could adapt to both weak acid environments. Compared to the conventional chemical reduction, bioreduction was considered as a sustainable route for producing CHBE under the eco-friendly performance condition [13].
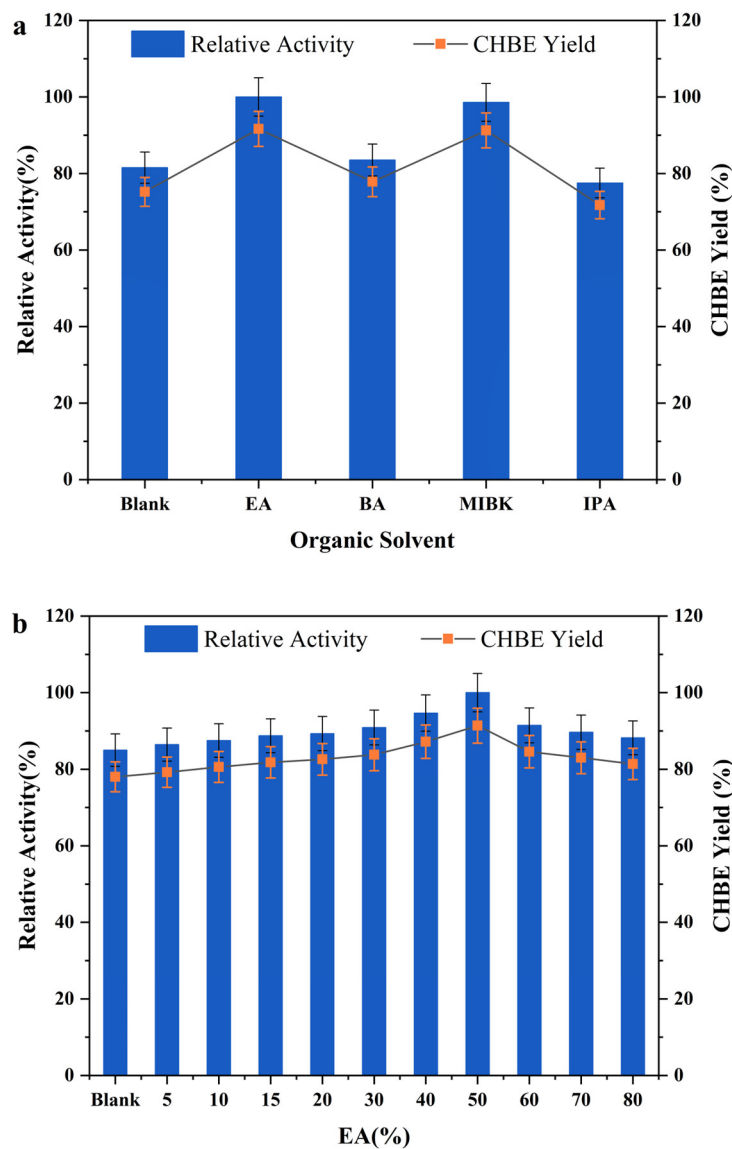

Figure 6. Effect of different organic solvents (50% of volumetric ratio) on the catalytic reaction (100 mM COBE, 30 °C, and pH 7.0) (**a**); effect of ethyl acetate (0–80% of volumetric ratio) on the catalytic reaction (100 mM COBE, 30 °C, and pH 7.0) (**b**).

CgCR was coexpressed with GDH to provide cofactor regeneration systems. Furthermore, the effects of co-substrate loading were assessed on the COBE-reducing activity. According to the results in Figure S1c (in Supplementary Materials), different ratios of glucose (glucose:COBE = 0.5:1, 1:1, 1.5:1, 2:1, 2.5:1, 3:1, 3.5:1, 4:1, or 5:1, molar ratio) were individually added into the bioreaction system. With the increase in glucose-to-COBE ratio from 0.5:1 to 3.5:1, the bioreaction efficiency displayed a slow rising trend and reached the maximum at the molar ratio of 3.5:1. From 4:1 to 5:1, the bioreaction efficiency showed a slow declining trend, indicating that the glucose reached saturation [67]. Metal ions might be associated with the enzyme configuration, and some metal ions would be coupled

with enzymes to alter the enzyme configuration, to promote or inhibit the biocatalytic efficiency [68]. The effects of different metal ions (6 mM) on biocatalytic reactions were studied. As displayed in Figure S2a (in Supplementary Materials), Cr^{3+}, Mg^{2+}, and Fe^{2+} inhibited the enzyme-catalyzed reaction. Other metal ions could promote the synthesis of COBE. Ni^{2+} had an apparent promotion effect. CoAKR7 was tolerant to most metal ions at a concentration of 5 mM [69], while the catalytic activity was completely inhibited by Fe^{2+} and Fe^{3+}.

Different concentrations of Ni^{2+} were selected to assess the effects of the biotransformation of COBE. The results are displayed in Figure S2b (in Supplementary Materials). As the Ni^{2+} concentration increased from 0 to 7 mM, the activities increased. Ni^{2+} (7 mM) could greatly enhance the COBE-reducing activity, and the highest yield of CHBE was over 80% in 1.5 h. After Ni^{2+} exceeded 7 mM, the biocatalytic activity was weakened. In the examination of some metal ions on the activity of *Anoxybacillus ayderensis* FMB1 reductase, there was an inhibitory effect of all metal ions on the bioreduction activity except Ca^{2+}, and Ca^{2+} increased the activity by 21% [70]. The effect of Ni^{2+} on the inhibition of FMB1 reductase reached 57%.

Substrate loading is a key factor in the biocatalytic reaction of industrialization [71]. Under the above-optimized bioreaction conditions, the influence of COBE concentration on the biocatalytic reaction was investigated (Figure S3, in Supplementary Materials). When the substrate concentration was 100 mM, COBE was fully reduced to CHBE within 3 h. Xu et al. investigated the effect of substrate concentration on the yield of the product [69]. When the substrate concentration was continuously increased to 100 mM, the highest product concentration of 77 mM (77% yield) was obtained after 28 h of the bioreaction. When the substrate concentration was 200–400 mM, CgCR could catalyze COBE to produce (*R*)-CHBE in a yield of 94% within 12 h. As COBE was 600–1000 mM, (*R*)-CHBE was produced in a yield of about 90% within 12 h. Accordingly, high substrate tolerance was found by using CgCR as a reductase biocatalyst.

3.3. Enhancement in COBE Bioreduction through Supply of Organic Solvent and Betaine/Lactic Acid

Organic solvents can enhance the biocatalytic efficiency [37]. To further improve the productivity of (*R*)-CHBE, an organic solvent–water system was constructed to improve the solubility of the substrate and product in the reaction system. The efficiency of four organic solvents (50%, v/v) (ethyl acetate (EA), butyl acetate (BA), isobutyl ketone (MIBK), and isopropyl alcohol (IPA)) was measured. These results are displayed in Figure 6a. In addition to IPA, compared with the blank group, the other three organic–aqueous systems had certain promoting effects, and the ethyl acetate (EA) aqueous system could give the highest catalytic efficiency. Shah constructed and applied a biphasic bioelectrocatalytic system [72]. To support the AdhS-catalyzed the bioconversion of COBE (100 mM) to (*R*)-CHBE for 10 h, the product yield reached only 85%. At the same substrate concentration, the bioreaction time was shorter in the EA-water system, while the yield of (*R*)-CHBE reached 91.5% within 0.5 h via the biocatalysis with CgCR cells. Compared with the aqueous system without organic solvents, the biocatalytic activity increased with the increase in the proportion of organic solvents, reaching the highest in the presence of EA (50 vol%), and the activity dropped when the loading of EA was over 50 vol% (Figure 6b). This suggests that the addition of organic solvents was beneficial to the stability of the enzyme to some extent [73]. Clearly, the optimal EA loading was 50 vol%.

To further enhance the (*R*)-CHBE yield, betaine/lactic acid was used as an additive in the EA-water system containing 50 vol% of EA. The effects of betaine/lactic acid loading on the biotransformation are shown in Figure 7. Upon raising the loading of betaine/lactic acid from 0 to 7 vol%, the COBE-reducing activities were raised. At 7 vol%, the COBE-reducing activities reached the maximum. After betaine/lactic acid exceeded 7 vol%, COBE-reducing activities began to decrease. Furthermore, 50 vol% of ethyl acetate, 7 vol% of betaine/lactic acid, and 43 vol% of water were mixed to construct the optimal bioreduction system, and

the yield of (*R*)-CHBE apparently increased compared to the single water system. This was probably related to the K-T parameters of the solution, which was used for estimating the chemical properties of reaction solutions. The corresponding parameters α, β, and π^* indicate the hydrogen-bonding acidity, basicity, and dipolarity/polarizability of the catalytic reaction solvent [27], respectively. A solution with a high α value might easily disrupt H-bonds to release H^+, while betaine/lactic acid with a high β value might have a high H-bond accepting ability. The α and β of betaine/lactic acid were 0.37 and 0.39, respectively, and the π^* value was 1.53. The α, β, and π^* of EA+H_2O were 0.39, 2.53, and 0.038, respectively, while the α, β, and π^* of EA+betaine/lactic acid+H_2O were 0.56, 1.77, and 0.27, respectively. Combined with the K-T parameters of betaine/lactic acid, the reason for increasing the yield of (*R*)-CHBE might be the increase in π^*. The high π^* value of the reaction system facilitated the COBE dissolution, which was more suitable for CgCR cells to participate in bioreduction.
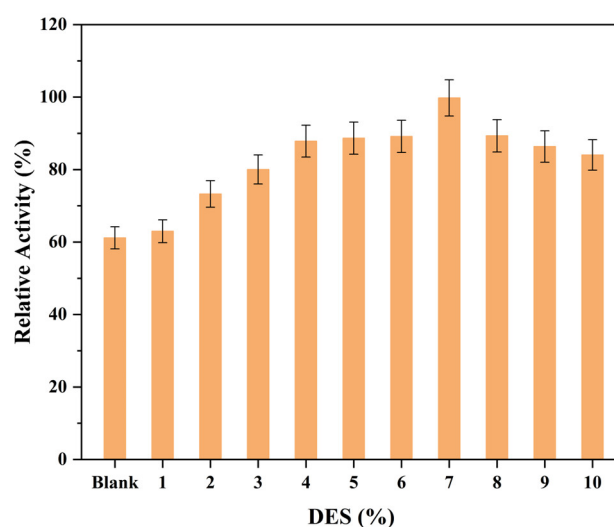

Figure 7. Effect of DES (betaine/lactic acid) loading on the biocatalytic reactions (100 mM COBE, 30 °C, and pH 7.0).

Accordingly, the optimal performance conditions were as follows: 30 °C; pH 7.0; co-substrate glucose, 3.5 mM glucose/mM COBE; metal ion additive Ni^{2+}, 7 mM; EA, 50 vol%; and betaine/lactic acid, 7 vol%. For the biotransformation of COBE into (*R*)-CHBE for 0.5 h, a high (*R*)-CHBE yield of 97.6% was obtained in the bioreaction system containing 7 vol% of betaine/lactic acid and 50 vol% of EA.

3.4. The Effect of Cell Permeability and Damage Degree on Biocatalysis

Additives (organic solvents, DES, etc.) might promote the catalytic reaction process [11,27,44]. They can promote the solubility of substrates and products. In addition, additives would increase the permeability of the whole cell by promoting the exchange process between cells and external substances. Some additives were selected to investigate the effects of different additives on cell permeability. As listed in Table S1 (in Supplementary Materials), OD_{260} and OD_{280} represent the content of proteins and DNA in the centrifugal supernatant, respectively. Without the additive (as a control), the organic solvent EA could promote the permeability of the CgCR cell membrane better than betaine/lactic acid. Notably, the combination of betaine/lactic acid plus EA might apparently enhance the permeability of the CgCR cell membrane. Increased permeability means that cell integrity is damaged [69]. To further investigate whether the effects of cell breakage and permeability on the catalytic bioreaction are related to each other, the catalytic reaction was investigated with cells of different breakage times. The results are shown in Figure S4 (in Supplementary Materials). After 15 min of crushing, the efficiency of the cell-catalyzed bioreaction was somewhat

enhanced, with a yield of 94.5% for CHBE. Over 30 min of crushing, the cell-catalyzed reaction decreased substantially.

The approach of coupling reductase with dehydrogenase for coenzyme regeneration is an efficient way to improve the bioreduction efficiency [74–76]. The asymmetric biosynthesis of (*R*)-CHBE from COBE was conducted through the bioreduction with CgCR cells containing CgCR and GDH in the presence of glucose. CgCR and GDH were used to build a double-enzymatic system for the regeneration of NADPH. Then, carbonyl reductase efficiently and asymmetrically synthesized (*R*)-CHBE from COBE, while glucose dehydrogenase utilized glucose to regenerate NADP$^+$ produced during COBE bioreduction. Accordingly, there was an efficient bioreduction of COBE to (*R*)-CHBE with CgCR cells in the EA-betaine/lactic acid-water system. The selected EA was easy to volatilize and separate for subsequent development and utilization. Betaine/lactic acid was easy to prepare as a green solvent. This developed strategy using EA and betaine/lactic acid as the cosolvent could enhance the catalytic efficiency. Considering the effects of other organic solvents or different types of DES might provide a broader perspective on the method's versatility. Long-term stability and repeatability tests would be beneficial to ensure the method's robustness over time. In future, it would be of great interest to develop a cost-effective catalysis process to enhance (*R*)-CHBE productivities with robust reductase biocatalysts in benign bioreaction medium.

4. Conclusions

Optically active (*R*)-CHBE is a key intermediate for the production of (*R*)-4-amino-3-hydroxy-butyric acid, *L*-carnitine, (*R*)-4-hydroxy-2-pyrrolidone, negamycin, and macrolactin A. To date, there has been great interest in the synthesis of (*R*)-CHBE from COBE through the bioreduction approach. CgCR was coexpressed with GDH to provide cofactor regeneration systems, and recombinant *E. coli* CgCR harboring NADPH-dependent reductase was created to efficiently transform the high loading of COBE into (*R*)-CHBE. At pH 7.0 and 30 °C, Ni^{2+} (7 mM) and glucose (3.5 mM glucose/mM COBE) were added into this bioreaction system containing COBE (1000 mM), and the (*R*)-CHBE yield reached about 90% within 12 h. The constructed EA-betaine/lactic acid-water (50:7:43 *v/v/v*) system could be used as optimal bioreaction medium for enhancing the bioreduction of COBE into (*R*)-CHBE (97.6% yield). The combination of betaine/lactic acid plus EA as the bioreaction medium could significantly improve the whole-cell permeability, which facilitated the bioreduction of COBE and enhanced the (*R*)-CHBE yield. Compared to other bioreduction approaches, this established bioreduction process could be used to synthesize (*R*)-CHBE in a high yield from 1000 mM COBE. This developed process shows high potential application in future.

References

1. Pinto, M.M.; Fernandes, C.; Tiritan, M.E. Chiral Separations in Preparative Scale: A Medicinal Chemistry Point of View. *Molecules* **2020**, *25*, 1931. [CrossRef] [PubMed]
2. Hancu, G.; Modroiu, A. Chiral Switch, between therapeutical benefit and marketing strategy. *Pharmaceuticals* **2022**, *15*, 240. [CrossRef] [PubMed]
3. Rahman, M.; Almalki, W.H.; Afzal, O.; Altamimi, A.S.A.; Ullah, S.N.M.N.; Barkat, M.A.; Beg, S. Chiral-engineered supraparticles, emerging tools for drug delivery. *Drug Discov. Today* **2022**, *28*, 103420. [CrossRef] [PubMed]
4. Antonopoulou, I.; Varriale, S.; Topakas, E.; Rova, U.; Christakopoulos, P.; Faraco, V. Enzymatic synthesis of bioactive compounds with high potential for cosmeceutical application. *Appl. Microbiol. Biotechnol.* **2016**, *100*, 6519–6543. [CrossRef] [PubMed]
5. Guo, Q.; Liang, S.; Xiao, Z.; Ge, C. Research progress on extraction technology and biological activity of polysaccharides from Edible Fungi: A review. *Food Rev. Int.* **2022**, *39*, 4909–4940. [CrossRef]
6. Fernandes, C.; Ribeiro, R.; Pinto, M.; Kijjoa, A. Absolute Stereochemistry Determination of Bioactive Marine-Derived Cyclopeptides by Liquid Chromatography Methods: An Update Review (2018–2022). *Molecules* **2023**, *28*, 615. [CrossRef] [PubMed]
7. Frontana-Uribe, B.A.; Little, R.D.; Ibanez, J.G.; Palma, A.; Vasquez-Medrano, R. Organic electrosynthesis, a promising green methodology in organic chemistry. *Green Chem.* **2010**, *12*, 2099–2119. [CrossRef]
8. He, T.; Wang, D.; Wu, Z.; Huang, C.; Xu, X.; Xu, X.; Liu, C.; Hashimoto, K.; Yang, C. A bibliometric analysis of research on (*R*)-ketamine from 2002 to 2021. *Neuropharmacology* **2022**, *218*, 109207. [CrossRef]
9. Wan, X.; Eguchi, A.; Fujita, Y.; Fujita, L.; Ma, X.; Wang, Y.; Yang, Y.; Qu, L.; Chang, J.; Zhang, C.; et al. Effects of (*R*)-ketamine on reduced bone mineral density in ovariectomized mice, A role of gut microbiota. *Neuropharmacology* **2022**, *213*, 109139. [CrossRef]
10. Pomara, C.; Cassano, T.; D'Errico, S.; Bello, S.; Romano, A.D.; Riezzo, I.; Serviddio, G. Data available on the extent of cocaine use and dependence, biochemistry, pharmacologic effects and global burden of disease of cocaine abusers. *Curr. Med. Chem.* **2012**, *19*, 5647–5657. [CrossRef] [PubMed]
11. Kasprzak, J.; Bischoff, B.; Becker, K.; Baronian, K.; Bode, R.; Schauer, F.; Vorbrodt, H.M.; Kunze, G. Synthesis of 1-(*S*)-phenylethanol and ethyl (*R*)-4-chloro-3-hydroxybutanoate using recombinant *Rhodococcus erythropolis* alcohol dehydrogenase produced by two yeast species. *Biochem. Eng. J.* **2016**, *106*, 107–117. [CrossRef]
12. Hoyos, P.; Pace, V.; Alcántara, A.R. Biocatalyzed synthesis of statins, A sustainable strategy for the preparation of valuable drugs. *Catalysts* **2019**, *9*, 260. [CrossRef]
13. Yang, Z.-Y.; Ye, W.-J.; Xie, Y.-Y.; Liu, Q.-H.; Chen, R.; Wang, H.-L.; Wei, D.-Z. Efficient asymmetric synthesis of ethyl (*S*)-4-chloro-3-hydroxybutyrate using alcohol dehydrogenase *Sm*ADH31 with high tolerance of substrate and product in a monophasic aqueous system. *Org. Process Res. Dev.* **2020**, *24*, 1068–1076. [CrossRef]
14. Kluson, P.; Stavarek, P.; Penkavova, V.; Vychodilova, H.; Hejda, S.; Jaklova, N.; Curinova, P. Stereoselective synthesis of optical isomers of ethyl 4-chloro-3-hydroxybutyrate in a microfluidic chip reactor. *J. Flow Chem.* **2019**, *9*, 221–230. [CrossRef]
15. Otani, Y.; Taguchi, A.; Hamada, K.; Hayashi, Y.; Yamaguchi, Y.; Baba, H. Influence of novel readthrough agents on myelin protein zero translation in the peripheral nervous system. *Neuropharmacology* **2022**, *211*, 109059. [CrossRef] [PubMed]
16. Purwadini, A.K.N.; Lusiani, C.E. Literature studt of *L*-carnitine preparation methods 1000 tons of annual production. *DISTILAT J. Teknol. Separasi* **2022**, *8*, 394–401. [CrossRef]
17. Tadiparthi, K.; Anand, P. A Journey toward the Syntheses of γ-Amino-β-hydroxybutyric Acid (GABOB) and Carnitine. *Org. Process Res. Dev.* **2021**, *25*, 2008–2019. [CrossRef]
18. Cano, A.; Turowski, P.; Ettcheto, M.; Duskey, J.T.; Tosi, G.; Sanchez-Lopez, E.; Garcia, M.L.; Camins, A.; Souto, E.B.; Ruiz, A. Nanomedicine-based technologies and novel biomarkers for the diagnosis and treatment of Alzheimer's disease, from current to future challenges. *J. Nanobiotechnol.* **2021**, *19*, 122. [CrossRef] [PubMed]
19. González De Aguilar, J.L. Lipid biomarkers for amyotrophic lateral sclerosis. *Front. Neurol.* **2019**, *10*, 284. [CrossRef]
20. Zhao, Q.; Fan, L.; Liu, Y.; Li, J. Recent advances on formation mechanism and functionality of chitosan-based conjugates and their application in o/w emulsion systems: A review. *Food Chem.* **2022**, *380*, 131838. [CrossRef]
21. Hamada, K.; Omura, N.; Taguchi, A.; Baradaran-Heravi, A.; Kotake, M.; Arai, M.; Takayama, K.; Taniguchi, A.; Roberge, M.; Hayashi, Y. New Negamycin-Based Potent Readthrough Derivative Effective against TGA-Type Nonsense Mutations. *ACS Med. Chem. Lett.* **2019**, *10*, 1450–1456. [CrossRef] [PubMed]
22. Lin, C.-K.; Tseng, P.-Y. Total synthesis of (–)-negamycin from a chiral advanced epoxide. *Synth. Commun.* **2023**, *53*, 119–126. [CrossRef]
23. Ghosh, S.; Das, S.; Ahmad, I.; Patel, H. In silico validation of anti-viral drugs obtained from marine sources as a potential target against SARS-CoV-2 Mpro. *J. Indian Chem. Soc.* **2021**, *98*, 100272. [CrossRef]

24. List, B.; Grossmann, O. Biocatalytic Reduction of Keto Esters and Heterocyclic Ketones in Continuous Flow. *Synfacts* **2020**, *16*, 1131. [CrossRef]

25. Kwon, J.H.; Lee, J.; Kim, J.; Kirchner, V.A.; Jo, Y.H.; Miura, T.; Kim, N.; Song, G.-W.; Hwang, S.; Lee, S.-G.; et al. Upregulation of Carbonyl Reductase 1 by Nrf2 as a Potential Therapeutic Intervention for Ischemia/Reperfusion Injury during Liver Transplantation. *Mol. Cells* **2019**, *42*, 672–685. [CrossRef]

26. Simić, S.; Zukić, E.; Schmermund, L.; Faber, K.; Winkler, C.K.; Kroutil, W. Shortening synthetic routes to small molecule active pharmaceutical ingredients employing biocatalytic methods. *Chem. Rev.* **2021**, *122*, 1052–1126. [CrossRef]

27. Kong, L.; Fan, B.; He, Y.-C. Efficient whole-cell biosynthesis of (*S*)-2-chloro-1-(3,4-difluorophenyl)-ethanol from 2-chloro-1-(3,4-difluorophenyl) ethanone in a sustainable reaction system. *Mol. Catal.* **2023**, *550*, 113570. [CrossRef]

28. Pennacchio, A.; Giordano, A.; Pucci, B.; Rossi, M.; Raia, C.A. Biochemical characterization of a recombinant short-chain NAD(H)-dependent dehydrogenase/reductase from *Sulfolobus acidocaldarius*. *Extremophiles* **2010**, *14*, 193–204. [CrossRef] [PubMed]

29. Zhu, J.; Bai, Y.; Fan, T.-P.; Zheng, X.; Cai, Y. Characterization of acid-resistant aldo–keto reductases capable of asymmetric synthesis of (*R*)-CHBE from *Lactobacillus plantarum* DSM20174. *Syst. Microbiol. Biomanuf.* **2022**, *3*, 634–646. [CrossRef]

30. Zhuang, W.; Liu, H.; Zhang, Y.; He, J.; Wang, P. Effective asymmetric preparation of (*R*)-1-[3-(trifluoromethyl) phenyl] ethanol with recombinant *E. coli* whole cells in an aqueous Tween-20/natural deep eutectic solvent solution. *AMB Express* **2021**, *11*, 118. [CrossRef] [PubMed]

31. Pan, L.; Li, Q.; Tao, Y.; Ma, C.; Chai, H.; Ai, Y.; He, Y.-C. An efficient chemoenzymatic strategy for valorisation of corncob to furfuryl alcohol in CA:Betaine-water. *Ind. Crops Prod.* **2022**, *186*, 115203. [CrossRef]

32. Qin, L.; Di, J.; He, Y. Efficient Synthesis of Furfuryl Alcohol from Corncob in a Deep Eutectic Solvent System. *Processes* **2022**, *10*, 1873. [CrossRef]

33. Jiang, W.; Pei, R.; Wu, W.; Zhao, P.; Tian, L.; Zhou, S.F. Catalytic site analysis and characterization of a solvent-tolerant aldo-keto reductase. *BioPharm Int.* **2019**, *32*, 34–40.

34. Dong, F.; Chen, H.; Malapit, C.A.; Prater, M.; Li, M.; Yuan, M.; Lim, K.; Minteer, S. Biphasic bioelectrocatalytic synthesis of chiral β-hydroxy nitriles. *J. Am. Chem. Soc.* **2020**, *142*, 8374–8382. [CrossRef]

35. Xie, P.; Zhou, X.; Zheng, L. Stereoselective synthesis of a key chiral intermediate of (*S*)-Rivastigmine by AKR-GDH recombinant whole cells. *J. Biotechnol.* **2019**, *289*, 64–70. [CrossRef] [PubMed]

36. Panić, M.; Bubalo, M.C.; Redovniković, I.R. Designing a biocatalytic process involving deep eutectic solvents. *J. Chem. Technol. Biotechnol.* **2021**, *96*, 14–30. [CrossRef]

37. Zhu, L.; Di, J.; Li, Q.; He, Y.-C.; Ma, C. Enhanced conversion of corncob into furfurylamine via chemoenzymatic cascade catalysis in a toluene–water medium. *J. Mol. Liq.* **2023**, *380*, 121741. [CrossRef]

38. Liang, S.; Wu, X.-L.; Xiong, J.; Zong, M.-H.; Lou, W.-Y. Metal–organic frameworks as novel matrices for efficient enzyme immobilization: An update review. *Coord. Chem. Rev.* **2020**, *406*, 213149. [CrossRef]

39. Wang, X.; Lan, P.C.; Ma, S. Metal-organic frameworks for enzyme immobilization, beyond host matrix materials. *ACS Cent. Sci.* **2020**, *6*, 1497–1506. [CrossRef]

40. Thangaraj, B.; Solomon, P.R. Immobilization of lipases–a review. Part I, enzyme immobilization. *ChemBioEng Rev.* **2019**, *6*, 157–166. [CrossRef]

41. Abbott, A.P.; Boothby, D.; Capper, G.; Davies, D.L.; Rasheed, R.K. Deep Eutectic Solvents Formed between Choline Chloride and Carboxylic Acids: Versatile Alternatives to Ionic Liquids. *J. Am. Chem. Soc.* **2004**, *126*, 9142–9147. [CrossRef] [PubMed]

42. Smith, E.L.; Abbott, A.P.; Ryder, K.S. Deep Eutectic Solvents (DESs) and Their Applications. *Chem. Rev.* **2014**, *114*, 11060–11082. [CrossRef]

43. Cao, J.; Wang, C.; Shi, L.; Cheng, Y.; Hu, H.; Zeng, B.; Zhao, F. Water based-deep eutectic solvent for ultrasound-assisted liquid–liquid microextraction of parabens in edible oil. *Food Chem.* **2022**, *383*, 132586. [CrossRef]

44. Li, Q.; Ma, C.-L.; He, Y.-C. Effective one-pot chemoenzymatic cascade catalysis of biobased feedstock for synthesizing 2,5-diformylfuran in a sustainable reaction system. *Bioresour. Technol.* **2023**, *378*, 128965. [CrossRef] [PubMed]

45. Cotroneo-Figueroa, V.P.; Gajardo-Parra, N.F.; López-Porfiri, P.; López-Porfiri, P.; Leiva, Á.; Gonzalez-Miquel, M.; Garrido, J.M.; Canales, R.I. Hydrogen bond donor and alcohol chain length effect on the physicochemical properties of choline chloride based deep eutectic solvents mixed with alcohols. *J. Mol. Liq.* **2022**, *345*, 116986. [CrossRef]

46. Bai, Y.; Zhang, X.-F.; Wang, Z.; Zheng, T.; Yao, J. Deep eutectic solvent with bifunctional Brønsted-Lewis acids for highly efficient lignocellulose fractionation. *Bioresour. Technol.* **2022**, *347*, 126723. [CrossRef] [PubMed]

47. Nian, B.; Cao, C.; Liu, Y. Synergistic Catalytic Synthesis of Gemini Lipoamino Acids Based on Multiple Hydrogen-Bonding Interactions in Natural Deep Eutectic Solvents-Enzyme System. *J. Agric. Food Chem.* **2020**, *68*, 989–997. [CrossRef] [PubMed]

48. Pätzold, M.; Siebenhaller, S.; Kara, S.; Liese, A.; Syldatk, C.; Holtmann, D. Deep eutectic solvents as efficient solvents in biocatalysis. *Trends Biotechnol.* **2019**, *37*, 943–959. [CrossRef] [PubMed]

49. Yang, D.; Zhao, N.; Tang, S.; Zhu, X.; Ma, C.; Fan, V.B.; Liang, J.; Yu, B.; Yang, L.; He, Y.C. A hybrid strategy for efficient valorization of bulrush into furoic acid in water-ChCl-based deep eutectic solvent. *Industrial Crops Prod.* **2022**, *177*, 114434. [CrossRef]

50. Sheldon, R.A.; Woodley, J.M. Role of Biocatalysis in Sustainable Chemistry. *Chem. Rev.* **2018**, *118*, 801–838. [CrossRef] [PubMed]

51. Xu, P.; Zheng, G.-W.; Zong, M.-H.; Li, N.; Lou, W.-Y. Recent progress on deep eutectic solvents in biocatalysis. *Bioresour. Bioprocess.* **2017**, *4*, 34. [CrossRef]

52. Yadav, N.; Venkatesu, P. Current understanding and insights towards protein stabilization and activation in deep eutectic solvents as sustainable solvent media. *Phys. Chem. Chem. Phys.* **2022**, *24*, 13474–13509. [CrossRef]
53. He, Y.-C.; Tao, Z.-C.; Zhang, X.; Yang, Z.-X.; Xu, J.-H. Highly efficient synthesis of ethyl (*S*)-4-chloro-3-hydroxybutanoate and its derivatives by a robust NADH-dependent reductase from *E. coli* CCZU-K14. *Bioresour. Technol.* **2014**, *161*, 461–464. [CrossRef]
54. Kolayli, S.; Keskin, M. Natural bee products and their apitherapeutic applications. *Stud. Nat. Prod. Chem.* **2020**, *66*, 175–196.
55. Li, Y.-Y.; Li, Q.; Zhang, P.-Q.; Ma, C.-L.; Xu, J.-H.; He, Y.-C. Catalytic conversion of corncob to furfuryl alcohol in tandem reaction with tin-loaded sulfonated zeolite and NADPH-dependent reductase biocatalyst. *Bioresour. Technol.* **2021**, *320*, 124267. [CrossRef]
56. Xiao, Z.; Zhong, W.; Liu, X. Recent developments in electrochemical investigations into iron carbonyl complexes relevant to the iron centres of hydrogenases. *Dalton Trans.* **2022**, *51*, 40–47. [CrossRef] [PubMed]
57. Yang, Z.; Fu, H.; Ye, W.; Xie, Y.; Liu, Q.; Wang, H.; Wei, D. Efficient asymmetric synthesis of chiral alcohols using high 2-propanol tolerance alcohol dehydrogenase SmADH2 via an environmentally friendly TBCR system. *Catal. Sci. Technol.* **2020**, *10*, 70–78. [CrossRef]
58. Chen, X.; Liu, Z.Q.; Lin, C.P.; Zheng, Y.G. Efficient biosynthesis of ethyl (*R*)-4-chloro3-hydroxybutyrate using a stereoselective carbonyl reductase from *Burkholderia gladioli*. *BMC Biotechnol.* **2016**, *16*, 70. [CrossRef] [PubMed]
59. Maugeri, Z.; Rother, D. Reductive amination of ketones catalyzed by whole cell biocatalysts containing imine reductases (IREDs). *J. Biotechnol.* **2017**, *258*, 167–170. [CrossRef] [PubMed]
60. Chen, Q.; Xie, B.; Zhou, L.; Maria-Solano, M.A.; Liu, W.D.; Li, J.; Feng, J.H.; Liu, X.T.; Osuna, S.; Guo, R.T.; et al. A tailor-made self-sufficient whole-cell biocatalyst enables scalable enantioselective synthesis of (*R*)-3-quinuclidinol in a high space-time yield. *Org. Process Res. Dev.* **2019**, *23*, 1813–1821. [CrossRef]
61. Gu, T.; Wang, B.; Zhang, Z.; Wang, Z.; Chong, G.; Ma, C.; Tang, Y.-J.; He, Y. Sequential pretreatment of bamboo shoot shell and biosynthesis of ethyl (*R*)-4-chloro-3-hydroxybutanoate in aqueous-butyl acetate media. *Process Biochem.* **2019**, *80*, 112–118. [CrossRef]
62. Lu, Y.; Dai, H.; Shi, H.; Tang, L.; Sun, X.; Ou, Z. Synthesis of ethyl (*R*)-4-chloro-3-hydroxybutyrate by immobilized cells using amino acid-modified magnetic nanoparticles. *Process Biochem.* **2022**, *99*, 9–20. [CrossRef]
63. Perveen, S.; Zhang, S.; Wang, L.; Ong, P.; Ouyang, Y.; Jiao, J.; Li, P. Synthesis of axially chiral biaryls via enantioselective ullmann coupling of ortho-chlorinated aryl aldehydes enabled by a chiral 2,2′-bipyridine ligand. *Angew. Chem. Int. Ed.* **2022**, *134*, e202212108. [CrossRef]
64. Liang, X.; Deng, H.; Xiong, T.; Bai, Y.; Fan, T.P.; Zheng, X.; Cai, Y. Overexpression and biochemical characterization of a carboxyspermidine dehydrogenase from *Agrobacterium fabrum* str. C58 and its application to carboxyspermidine production. *J. Sci. Food Agric.* **2022**, *102*, 3858–3868. [CrossRef] [PubMed]
65. Xia, Q.; Liu, Y.; Meng, J.; Cheng, W.; Chen, W.; Liu, S.; Liu, Y.; Li, J.; Yu, H. Multiple hydrogen bond coordination in three-constituent deep eutectic solvents enhances lignin fractionation from biomass. *Green Chem.* **2018**, *20*, 2711–2721. [CrossRef]
66. Luo, W.; Du, H.-J.; Bonku, E.M.; Hou, Y.-L.; Li, L.-L.; Wang, X.-Q.; Yang, Z.-H. An Alkali-tolerant Carbonyl Reductase from *Bacillus subtilis* by Gene Mining: Identification and Application. *Catal. Lett.* **2019**, *149*, 2973–2983. [CrossRef]
67. Yuan, L.; Qin, Y.-L.; Zou, Z.-C.; Appiah, B.; Huang, H.; Yang, Z.-H.; Qun, C. Enhancing intracellular NADPH bioavailability through improving pentose phosphate pathway flux and its application in biocatalysis asymmetric reduction reaction. *J. Biosci. Bioeng.* **2022**, *134*, 528–533. [CrossRef] [PubMed]
68. Plž, M.; Petrovičová, T.; Rebroš, M. Semi-continuous flow biocatalysis with affinity co-immobilized ketoreductase and glucose dehydrogenase. *Molecules* **2020**, *25*, 4278. [CrossRef] [PubMed]
69. Zhang, Y.; Duan, Y.; Zhong, L.; Li, Z.; Cui, Z.; Huang, Y. Characterization of a novel aldo-keto reductase with anti-Prelog stereospecificity from *Corallococcus* sp. EGB. *Int. J. Biol. Macromol.* **2020**, *146*, 36–44. [CrossRef]
70. Xu, S.; Lin, Q.; Chen, W.; Lin, R.; Shen, Y.; Tang, P.; Yu, S.; Du, W.; Li, J. Efficient Biosynthesis of (*S*)-1-chloro-2-heptanol Catalyzed by a Newly Isolated Fungi *Curvularia hominis* B-36. *Catalysts* **2022**, *13*, 52. [CrossRef]
71. Bekler, F.M.; Güven, K.; Gül Güven, R. Purification and characterization of novel α-amylase from *Anoxybacillus ayderensis* FMB1. *Biocatal. Biotransform.* **2021**, *39*, 322–332. [CrossRef]
72. Bu, C.; Qiao, H.; Zou, L.; Tao, Y.; Fu, J.; Liu, C.; Zheng, Z.; Ouyang, J. Hydrogenation of biomass pyrolysis oil using enhanced reduction catalytic capacity cellular by expressing excavated carbonyl reductase. *Fuel* **2023**, *332*, 126108. [CrossRef]
73. De Gonzalo, G.; Alcántara, A.R.; de María, P.D.; Sánchez-Montero, J.M. Biocatalysis for the asymmetric synthesis of Active Pharmaceutical Ingredients (APIs): This time is for real. *Expert Opin. Drug Discov.* **2022**, *17*, 1159–1171. [CrossRef] [PubMed]
74. Shah, S.; Sunder, A.V.; Singh, P.; Wangikar, P.P. Characterization and Application of a Robust Glucose Dehydrogenase from Paenibacillus pini for Cofactor Regeneration in Biocatalysis. *Indian J. Microbiol.* **2020**, *60*, 87–95. [CrossRef] [PubMed]
75. Di, J.; Liao, X.; Li, Q.; He, Y.-C.; Ma, C. Significantly enhanced bioconversion of high titer biomass-derived furfural to furfuryl alcohol by robust endogenous aldehyde reductase in a sustainable way. *Green Chem.* **2023**, *in press*. [CrossRef]
76. Ye, Q.; Ouyang, P.K.; Ying, H.J. A review—biosynthesis of optically pure ethyl (*S*)-4-chloro-3-hydroxybutanoate ester: Recent advances and future perspectives. *Appl. Microbiol. Biotechnol.* **2011**, *89*, 513–522. [CrossRef]